Research article

A versatile 2A peptide-based strategy for ectopic expression and endogenous gene tagging in *Trypanosoma cruzi*

Gabriela T. Niemirowicz [1], Giannina Carlevaro [1], Oscar Campetella, León A. Bouvier [**], Juan Mucci [*]

Instituto de Investigaciones Biotecnológicas, Consejo Nacional de Investigaciones Científicas y Técnicas (CONICET). Universidad Nacional de San Martín–Escuela de Bio y Nanotecnologías (EByN). Campus Miguelete, 25 de Mayo y Francia (B1650HMP), San Martín, Argentina

A B S T R A C T

Nearly all expression vectors currently available for *Trypanosoma cruzi* were conceived to produce a single primary transcript containing the genes of interest along with those that confer antibiotic resistance. However, since each messenger RNA (mRNA) matures separately, drug selection will only guarantee the expression of those derived from the selectable marker. Therefore, commonly a considerable fraction of the cells recovered after selection with these expression vectors, although resistant do not express the protein of interest. Consequently, in order to counteract this disadvantage, we developed vectors with an alternative arrangement in which the gene of interest and antibiotic resistance are fused sharing the same mRNA. To test this configuration, we included the coding sequence for the green fluorescent protein (mEGFP) linked to the one conferring neomycin resistance (Neo). Additionally, to allow for the production of two independent proteins the sequence for a *Thosea asigna* virus self-cleaving 2A peptide (T2A) was inserted in-between. Cells obtained with these vectors displayed higher mEGFP expression levels with more homogeneous transgenic parasite populations than those transfected with more conventional independent mRNA-based alternatives. Moreover, as determined by Western blot, 2A mediated fusion protein dissociation occurred with high efficiency in all parasite stages. In addition, these vectors could easily be transformed into endogenous tagging constructs that allowed the insertion, by ends-in homologous recombination, of a hemagglutinin tag (HA) fused to the *actin* gene. The use of 2A self-cleaving peptides in the context of single mRNA vectors represents an interesting strategy capable of improving ectopic transgene expression in *T. cruzi* as well as providing a simple alternative to more sophisticated methods, such as the one based on CRISPR/Cas9, for the endogenous labeling of genes.

1. Introduction

Chagas disease, also known as American trypanosomiasis, is a zoonotic infection caused by the protozoan flagellate *Trypanosoma cruzi*. This disease affects almost 7 million people worldwide and is endemic in Mexico, Central, and South America. However, given the mild symptoms associated to the acute stage of Chagas disease, new cases often go unrecognized. Approximately 60–90 days post-infection, individuals progress to the chronic stage. Throughout their lives, around 30 % of patients will develop clinical manifestations such as cardiac, digestive (megacolon or megaesophagus), or neurological issues. Moreover, since no effective drugs are available for the chronic phase, these pathologies often trigger severe disabilities requiring the allocation of substantial resources for treatment, and in some cases, even death. In this context, functional genomics approaches are extremely valuable to understand essential mechanisms of *T. cruzi* biology, which may eventually lead to the development of new chemotherapeutic strategies.

T. cruzi, as well as other kinetoplastids, exhibits a distinctive genomic organization. Genes for unrelated proteins are arranged in

---

long units sharing the same orientation with intergenic regions located in-between. Although gene expression involves transcription of these clustered arrangements by RNA polymerase II, their regulation is mostly accomplished at the post-transcriptional level [1]. Each individual mRNA derives from the primary polycistronic transcripts by the co-transcriptional action of the *trans*-spliceosome. Centered around the transcribed intergenic region this complex is responsible for the addition, by *trans*-splicing, of a short-capped RNA to the 5′ end of the downstream coding sequence as well as the polyadenylation of the preceding gene located upstream [2,3]. Both un-translated regions (UTRs) flanking the coding sequence in the resulting mature mRNAs can bind different regulatory proteins that influence messenger stability, translation efficiency, steady-state levels, and localization. Consequently, intergenic sequences stand out as key elements that govern stage specific gene expression patterns as well as expression level modulation in response to changes in the environment [1,4]. For this reason, to ensure transgene expression in all developmental stages, kinetoplastid genetic manipulation constructs usually include intergenic regions derived from housekeeping genes. In this sense, the pTEX vector, the first *T. cruzi* episomal plasmid described, was constructed with intergenic sequences of the glyceraldehyde 3-phosphate dehydrogenase (GAPDH) locus with the *neomycin phosphotransferase* gene (*Neo*) providing G418 resistance [5]. Due to the post-transcriptional nature of gene expression regulation, any processive RNA polymerase can be used to drive transgene expression. Therefore, later designs employed RNA polymerase I (RNAPI) ribosomal promoters to enhance expression levels [6,7]. These elements also confer integrative properties since circular molecules with rRNA promoters recombine into ribosomal loci [8]. Similarly, the inclusion of a section of a beta-tubulin gene has allowed the stable insertion of constructs into the tubulin locus by ends-in homologous recombination [9]. In more recent years, extended sets of selectable markers and reporter genes in episomal as well as integrative DNA contexts have been made available [10]. Systems based on T7 or RNAPI promoters combined with tetracycline-responsive elements also were developed allowing the exogenous control of gene expression [11,12].

Lately, genetic manipulation of *T. cruzi* has extensively been focused on CRISPR/Cas9 based genome editing methodologies [13]. However, conventional and more accessible methods to express transgenes are still laborious and time-consuming [14]. In particular, drug selection in *T. cruzi* is usually a lengthy process requiring at least one month. Frequently, after selection, a considerable fraction of the cells recovered, although resistant do not express the gene of interest nor exhibit the desired genomic modification [15–18]. This phenomenon can be attributed in part to the ability of *T. cruzi* to maintain exogenous genetic material as episomes with autonomous extrachromosomal replication [5]. Alternatively, it might be related to the multi-messenger design of most available gene expression and manipulation tools. Although the same primary transcript gives rise to the mRNAs for the genes of interest as well as the selectable marker, each molecule matures independently and therefore, as long as the expression of the resistance gene is preserved, the rest of the construct might be subject of disabling mutations, deletions, or rearrangements. This is particularly prevalent when the experimental methodologies involve the expression of transgenes with detrimental effects on cellular viability or after maintaining the cells for extended periods in culture. Similar shortcomings have been observed in diverse genetic systems developed for different organisms and cellular models. In many cases, the use of 2A self-cleaving peptides, enabling the simultaneous expression of multiple genes, helped overcome these limitations. Briefly, 2A peptides were originally described in mammalian viruses of the *Picornaviridae* family, including aphtho- (foot-and-mouth disease viruses and equine rhinitis A virus), and cardioviruses (encephalomyocarditis virus). These sequences are short (usually 19–22 amino acids) and "auto separate" the viral polyproteins during translation. This mechanism involves ribosomal stalling and skipping of the formation of a glycyl-prolyl peptide bond at the C-terminus of a highly conserved sequence shared by different 2As, the GDVEXNPGP motif, and leads to the production of different proteins with equimolar stoichiometry [19,20]. In this sense, several strategies have exploited this principle to express two or more independent proteins from a single mRNA such as the generation of monoclonal antibodies [21,22], gene therapy approaches [23] or the production of β-carotene in rice [24]. Moreover, the reduced number of regulatory elements required to produce multiple proteins has made feasible the expression of
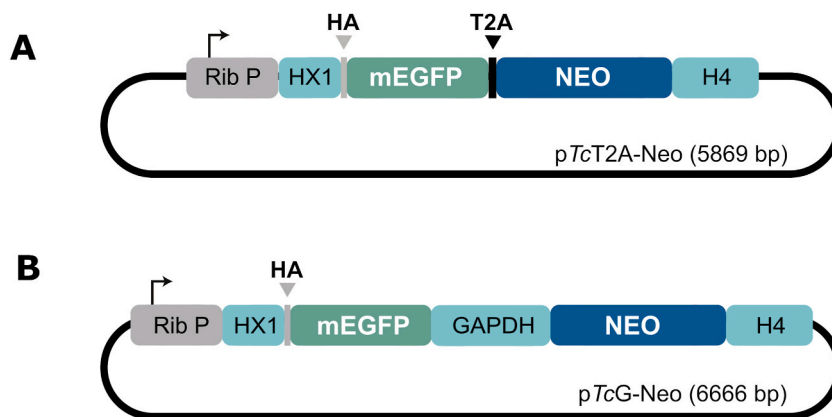

Fig. 1. Schematic diagram of pTcT2A-Neo and pTcG-Neo vectors. (A) The *T. asigna* virus 2A-like peptide sequence (T2A) was inserted between a *mEGFP* reporter and a G418 resistance (*Neo*) gene. Transcription of the 2A-linked construct is driven by an rRNA promoter (Rib. P). The HX1 and *histone H4* intergenic regions were included on either side of the coding sequence for mRNA maturation. (B) The section containing the T2A coding sequence was replaced with a *GAPDH* intergenic region to obtain a plasmid with a conventional multi mRNA configuration. Alternatively, to monitor mEGFP expression, a hemagglutinin (HA) tag was added to the N-terminus of the reporter.

A

B
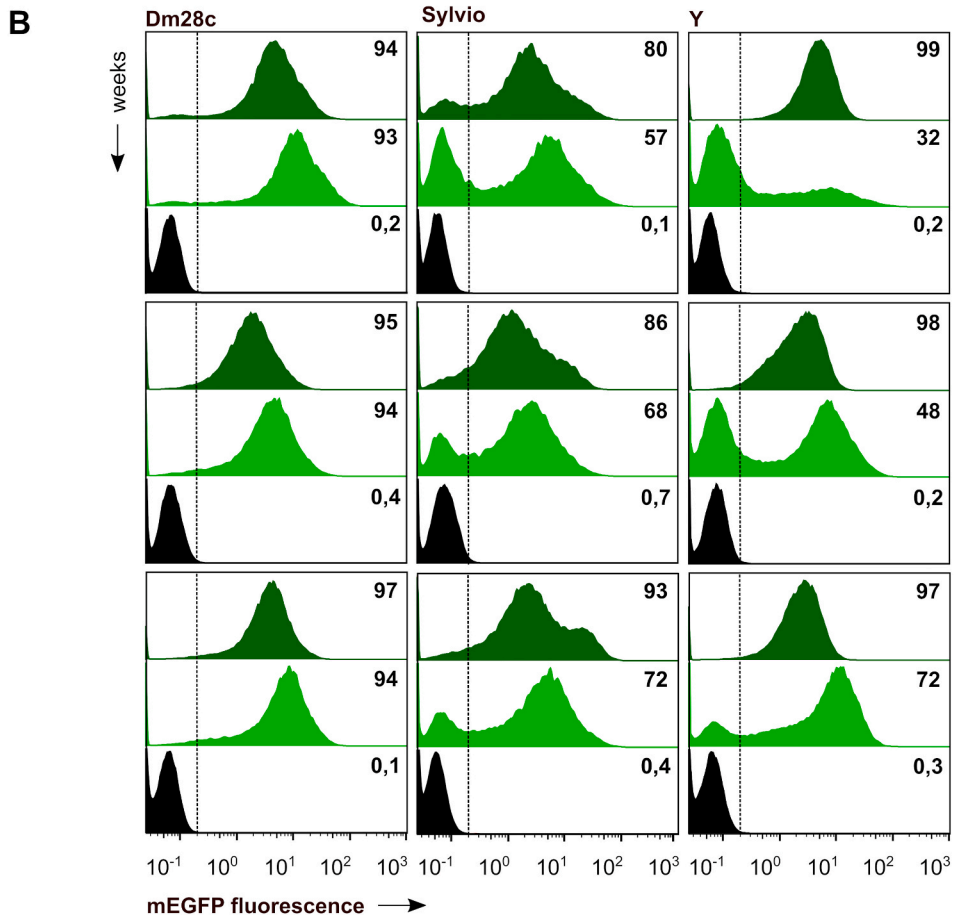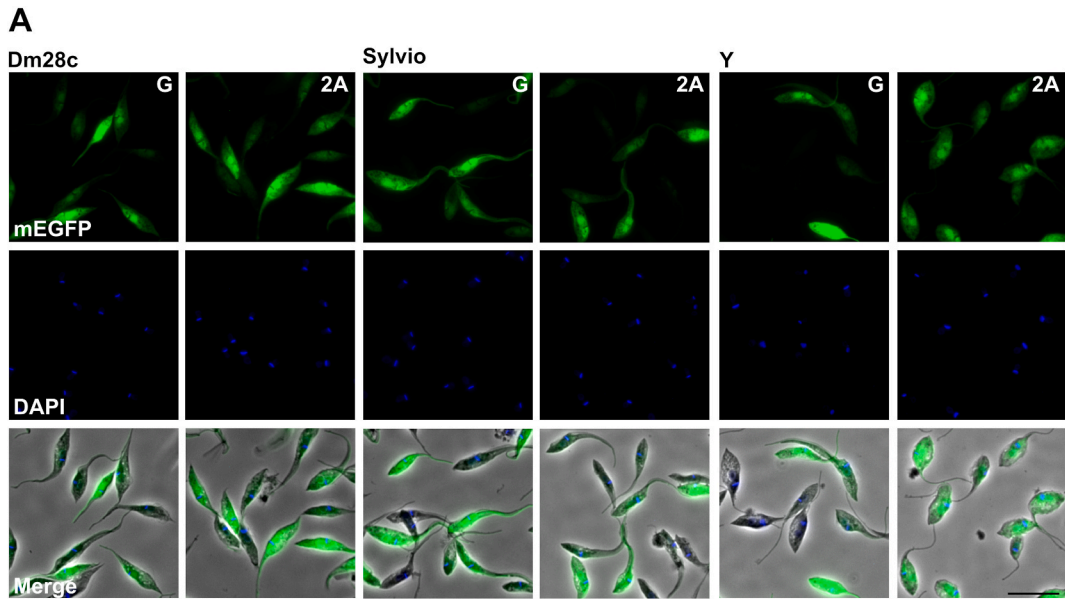
(caption on next page)

Fig. 2. mEGFP expression in *T. cruzi* epimastigotes. (A) Images of Dm28c, Sylvio-X10 and Y epimastigotes transfected with p*Tc*T2A-Neo (2A) and p*Tc*G-Neo vectors (G). Scale bar: 10 μm. (B) Fixed p*Tc*T2A-Neo (green) and p*Tc*G-Neo (light green) transfected parasites were analyzed by flow cytometry 4-, 8- and 12-weeks post transfection. For comparative purposes the mEGFP positive cell fraction is indicated in the upper right edge of each histogram. Parental strains are depicted in black. (For interpretation of the references to colour in this figure legend, the reader is referred to the Web version of this article.)

entire metabolic pathways from a single promoter [25]. Due to their small size, 2A peptide fusions normally do not interfere significantly with the function and structure of proteins and given that the ribosomal stalling and skipping phenomena only depend on the highly conserved eukaryotic ribosome, they have been successfully used in different cell types.

In *T. cruzi*, viral like functional self-cleaving 2A sequences have been described in genes associated with L1Tc non-LTR retro-transposons. Most of these elements maintain the canonical 2A motif and, noteworthy, are always located in frame at the N-terminus of the proteins encoded by L1Tc [26]. Self-cleaving 2A peptides have been included in genetic constructs for functional complementations and CRISPR/Cas9 associated homology-directed repair templates in this organism [27–29]. However, to date, the advantage of using these elements has not been thoroughly analyzed. In this work, we compare the performance of conventional multi mRNA and 2A based vectors for the expression of fluorescent reporter genes targeted to the cytosol or the nucleus. Additionally, we explore the feasibility of adapting this strategy for the efficient endogenous tagging of the *actin* gene.

2. Results

2.1. Plasmid description

To assess the performance of expressing a protein of interest fused, through a 2A peptide, to a selectable marker, two vectors were
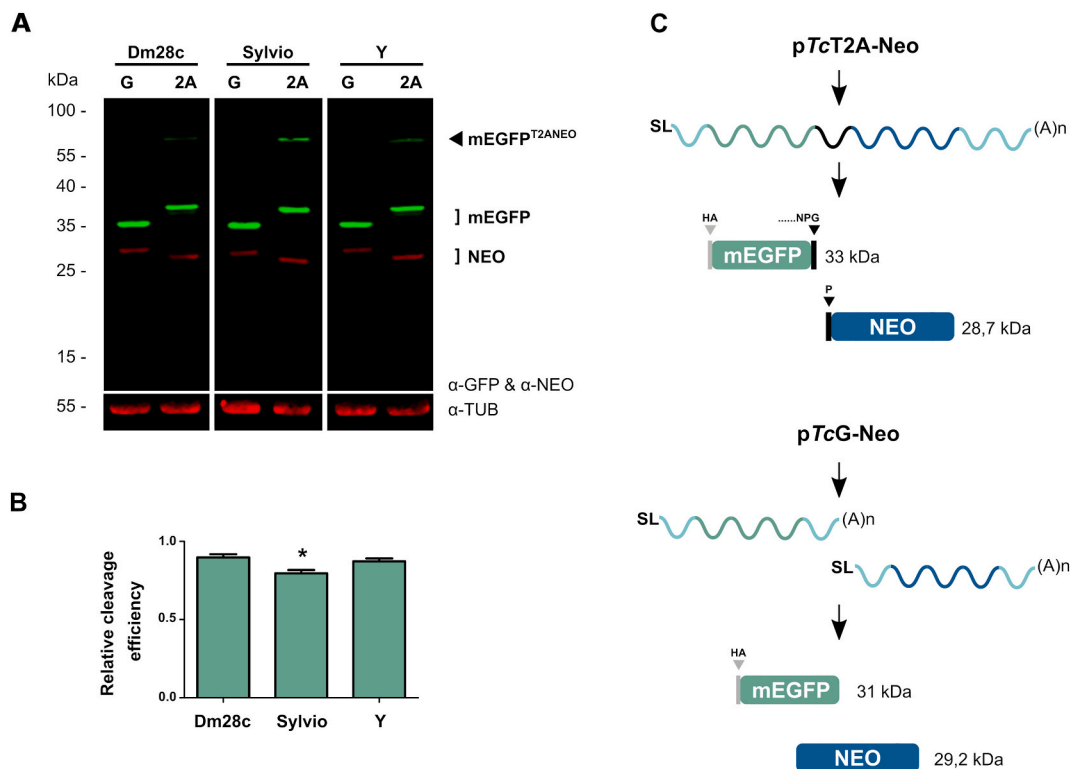

Fig. 3. Cleavage efficiency of T2A in *T. cruzi* epimastigotes. (A) mEGFP and *Neo* expression levels were monitored 5 weeks post transfection by Western blot analysis in total cell extracts (5×10^6 cells per lane). Tubulin was used as a loading control. Full image can be found in Supplementary Fig. 5 (B) Relative cleavage efficiencies for mEGFP^{T2ANeo} polyprotein were: Dm28c, 90 ± 2 %; Sylvio-X10 80 ± 2 % and Y, 87 ± 2 % (n = 3). (C) The p*Tc*T2A-Neo vector enables the expression of multiple polypeptides from a single mRNA molecule. During translation, ribosomal skipping results in production of two independent proteins. The 20 first amino acids of the cleaved T2A peptide remains fused to the C-terminus of the mEGFP protein, while a Pro residue is added to the N-terminus of the neomycin phosphotransferase enzyme (Neo). For comparative purposes the conventional two-mRNA derivative p*Tc*G-Neo plasmid is shown in the figure. Messenger RNAs are depicted with spliced leader (SL) and polyA tail (A)$_n$. Differences between the observed (A) and predicted (C) molecular weights of the mEGFP variants where noted. These could be attributed to different factors such as specific residue composition of the fusion proteins or to inaccuracies in the reported molecular weight correspondence of the pre-stained standard [54].

developed. To obtain p*Tc*T2A-Neo (Fig. 1A), the coding sequence for a *Thosea asigna virus* 2A-like peptide (T2A) [30] was inserted between the green fluorescent protein (mEGFP) reporter and a downstream G418 resistance gene (*Neo*) coding sequence. The starting ATG codon of the later was removed to prevent any independent translation initiation. Transcription is driven by an rRNA promoter [6] and the HX1 [7] and histone H4 intergenic regions were included on either side of the coding sequence for mRNA maturation. As a control for this single mRNA vector, p*Tc*G-Neo (Fig. 1B) was derived with a more conventional configuration. Essentially, the section containing the T2A coding sequence was replaced with a *GAPDH* intergenic region [5] which included appropriate stop and ATG translation initiation codons for the *mEGFP* and *Neo* genes, respectively.

2.2. mEGFP expression in T. cruzi

T. cruzi is a genetically and phenotypically diverse species [31] with broad variability with respect to, for example, strain morphology [32], degree of virulence and lethality [33], tropism [34] and drug sensitivity [35]. Consequently, different aspects of the biology of this organism are studied employing specific model strains. Therefore, we compared the performance of each vector configuration in different strains by transfection of both constructs into Dm28c, Sylvio-X10 and Y epimastigotes. After four weeks of selection, microscopic examination revealed fluorescent cells in all six cultures with mEGFP signal evenly distributed throughout the cell body (Fig. 2A). Population heterogeneity, as determined by flow cytometry, showed differences between lines obtained with each
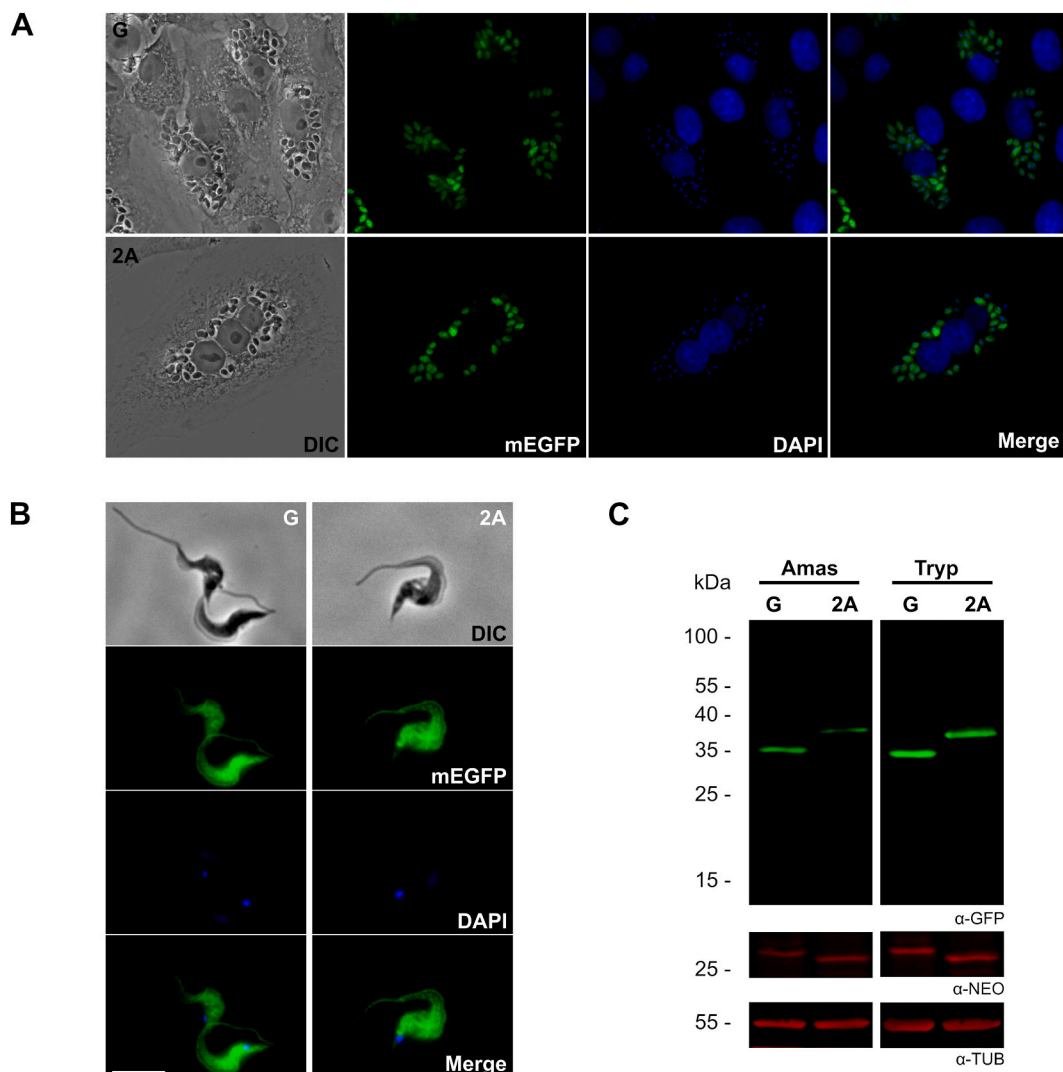

Fig. 4. p*Tc*T2A-Neo vector can drive mEGFP expression in amastigote and trypomastigote cells. (A) Sylvio-X10 amastigote-infected Vero cells fixed 72 h post infection. (B) Tissue culture-derived trypomastigotes. DNA was stained with DAPI. Scale bar: 5 μm (C) T2A processing was monitored by Western blot analysis in total cell extracts of isolated intracellular amastigotes (Amas) and cell culture-derived trypomastigotes (Tryp) (1×10^7 cells per lane). Tubulin was used as a loading control. Full images can be found in Supplementary Fig. 5.

vector and among different strains as well, which is in accordance with previous reports [36]. Both vectors yielded equally homogeneous all-fluorescent Dm28c epimastigote populations. This feature was maintained throughout the three months these cells were kept in culture. On the other hand, in Sylvio-X10 and especially in Y strain cells, p*Tc*T2A-Neo outperformed the two-mRNA derivative. Populations obtained with the former reached higher fractions of fluorescent cells with fewer passages and shorter time in culture (Fig. 2B). Regarding T2A self-cleavage efficiency, Western-blot analysis showed a high percentage of processing in all three strains (Fig. 3A) with >80 % of processed fusion protein as determined by band quantification (Fig. 3B). Remnants of the T2A peptide extending from the C-terminus of mEGFP in these cell lines could be noticed as a 2 kDa molecular weight increase when compared to that expressed in strains transfected with p*Tc*G-Neo (Fig. 3C). As an additional processing control, the antibiotic resistance protein expression was also analyzed. Perceived differences in *Neo* gene product motility were due to the omission of N-terminus residues, dispensable for G418 resistance, during the construction of the single mRNA variant.

In order to evaluate T2A processing in other stages, Vero cells were infected with transgenic Sylvio-X10 strain metacyclic trypomastigotes, derived by spontaneous differentiation of the corresponding epimastigotes. As seen by fluorescence microscopy, both types of plasmids yielded intracellular amastigotes as well as culture trypomastigotes with uniform mEGFP distribution (Fig. 4A and B). Extracts recovered from these stages were analyzed by Western blot revealing reporter and resistance protein expression patterns comparable to those previously observed in samples derived from their respective epimastigote counterparts (Fig. 4C). Noteworthy, no bands corresponding to the unprocessed fusion protein could be detected which might suggest more efficient T2A self-cleavage in these vertebrate host associated stages.

2.3. Improved nuclear mEGFP expression

To assess the possibility of employing the T2A based approach for the expression of proteins targeted to subcellular compartments other than the cytosol, plasmids were modified in order to express mEGFP fused to nuclear localization signals (NLS) (Fig. 5A). Initially, the sequence for a single *T. cruzi* La protein NLS [37] was placed immediately downstream of the *mEGFP* gene found in both
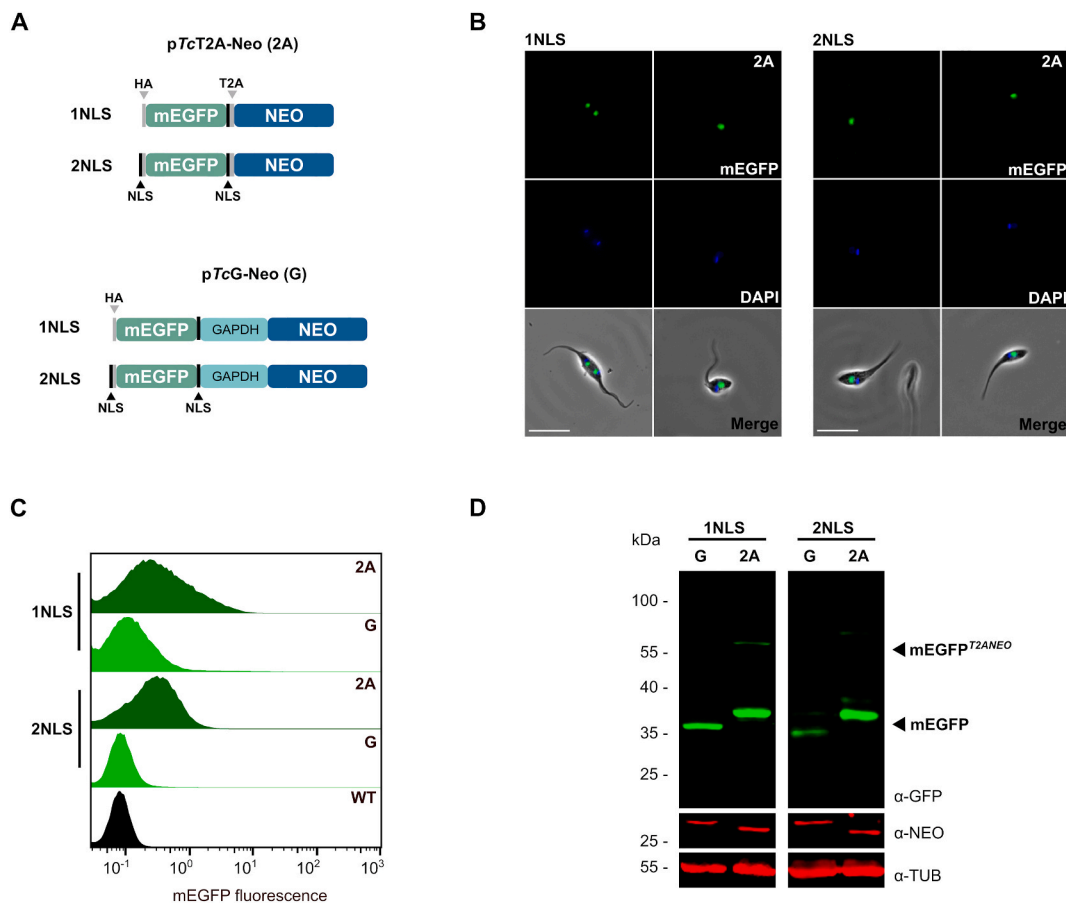

Fig. 5. Improved nuclear mEGFP expression through 2A strategies. (A) Schematic representation of different constructs coding for a mEGFP fused to the La protein nuclear localization signal. (B) Images of Sylvio-X10 cells. Parasite DNA was stained with DAPI. Scale bar: 10 μm (C) mEGFP expression of fixed parasites was analyzed by flow cytometry 4 weeks post transfection. (D) T2A processing was monitored by Western blot analysis in total cell extracts (5 × 10^6 cells per lane). Tubulin was used as a loading control. Full images can be found in Supplementary Fig. 5.
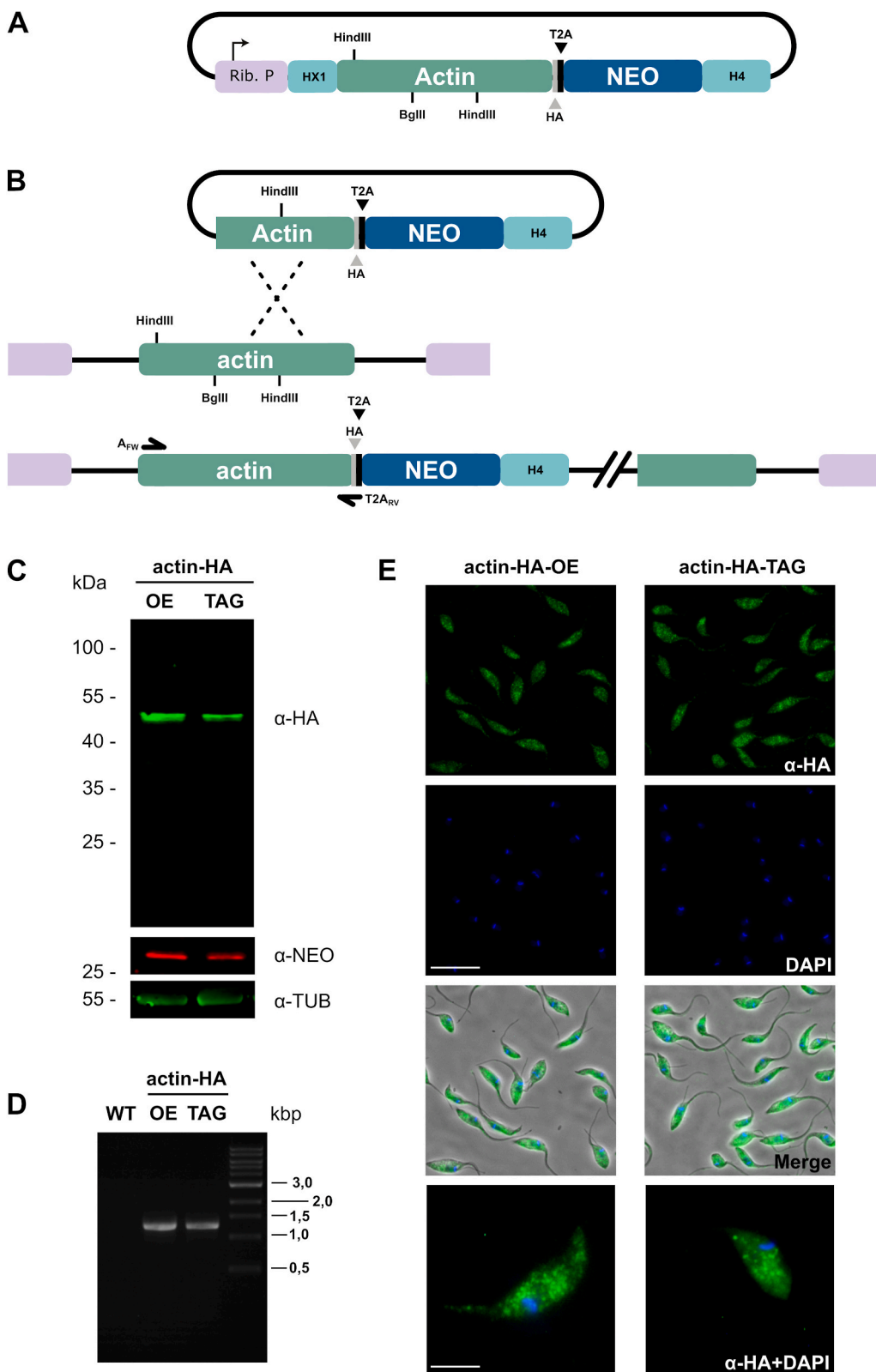
(caption on next page)

Fig. 6. T2A peptide mediated endogenous *actin* gene tagging. (A) Schematic representation of p*Tc*T2A-*actin*-HA (OE) plasmid. (B) p*Tc*T2A-*actin*-HA was modified removing the ribosomal promoter, the HX1 splice acceptor site and the initial 254 bp segment of the *actin* gene to produce the endogenous tagging derivative. Construct insertion by ends-in homologous recombination can be analyzed by PCR employing the depicted primers. (C) HA endogenously tagged actin (TAG) and actin-HA overexpression (OE) was monitored by Western blot analysis in total cell extracts (5×10^6 cells per lane). Tubulin was used as a loading control. Full images can be found in Supplementary Fig. 5 (D) PCR analysis using gDNA isolated from wild type (WT), TAG and OE parasites. (E) Immunofuorescence microscopy images probed with anti-HA primary antibody. Parasite DNA was stained with DAPI. Scale bars: panels, 10 μm; Magnification, 5 μm.

types of vectors. The mEGFP-NLS fusion protein expressed with p*Tc*T2A-Neo would have a C-terminus extension comprised of T2A derived residues. Given that this extension might interfere with nuclear targeting thus likely affecting comparative vector performance evaluation, a supplementary pair of plasmids was obtained. In these the sequence for an additional La protein NLS was inserted upstream of the *mEGFP* gene (Fig. 5A). All four resulting plasmids were transfected into Sylvio-X10 epimastigotes which were kept under selection for one month. After this period, transgenic cells with nuclear targeted mEGFP could be detected by epifluorescence microscopy in each corresponding culture (Fig. 5B). No localization differences could be found between fusion proteins containing single or double NLS nor was there any effect of C-terminal T2A remaining on NLS targeting function.

Flow cytometry showed that both vectors derived from p*Tc*T2A-Neo performed far better than their respective counterparts obtained with p*Tc*G-Neo yielding significantly higher ratios of fluorescent parasites (Fig. 5C). These differences also were apparent when mEGFP reporter expression was analyzed by Western blot (Fig. 5D).

2.4. T2A peptide mediated endogenous actin gene tagging

To analyze the feasibility of expressing endogenous genes with a T2A peptide-based strategy, the sequence corresponding to mEGFP in p*Tc*T2A-Neo was replaced with a Dm28c strain derived *actin* gene fused to a C-terminus HA tag, yielding plasmid p*Tc*T2A-*actin*-HA (Fig. 6A). In addition, this vector was further modified by removing the ribosomal promoter, the HX1 splice acceptor site and the initial 254 bp segment of the *actin* gene to produce p*Tc*EndoT2A-*actin*-HA. Without these regulatory elements, expression of the *Neo* gene would hardly be possible and therefore the occurrence of resistant parasites maintaining this construct as an episome would be highly infrequent. However, linearization at the *actin* gene derived sequence targets this construct for integration into the *actin* locus by ends-in homologous recombination [38]. Thus, the cells would not only acquire G418 resistance but also express an endogenously HA tagged *actin* gene (Fig. 6B). Dm28c strain epimastigotes were transfected with circular p*Tc*T2A-*actin*-HA and *Hind*III linearized p*Tc*EndoT2A-*actin*-HA and kept under selection for two months to increase the likelihood of recovering homogeneous transgenic parasite populations. Western blot analysis of extracts derived from cells obtained with p*Tc*T2A-*actin*-HA revealed a band that matched the predicted 46 kDa of the recombinant actin-HA fusion protein (Fig. 6C). Likewise, a band with identical molecular weight could be observed in samples from parasites transfected with p*Tc*EndoT2A-*actin*-HA, suggesting that the vector had indeed been inserted into the *actin* locus restoring the full length of the gene. Noteworthy, no additional bands could be detected in this extract, indicating that no viable construct rearrangement, recircularization, or random insertion had taken place in a significant fraction of the transgenic parasites obtained. Relating to the different regulatory elements involved in each case, band quantification revealed that recombinant actin-HA fusion and Neo resistance proteins were respectively ∼30 % and ∼45 % less abundant in cells expressing from the endogenous locus than in those where the transgenes were expressed ectopically with p*Tc*T2A-*actin*-HA. On the other hand, bands corresponding to unprocessed T2A fusion proteins remained under the level of detection.

To further confirm that an *actin* gene had endogenously been tagged with p*Tc*EndoT2A-*actin*-HA, genomic DNA was purified and analyzed by PCR with primer pairs that hybridize to the 5′ end of the *actin* gene and the sequence coding for the T2A peptide (Fig. 6D). Positive control reactions were carried out on DNA from parasites transfected with p*Tc*T2A-*actin*-HA. Amplification products obtained from both samples agreed with the predicted 1238 bp size indicating that the construct had indeed integrated into the *actin* locus (Fig. 6D).

Flow cytometry of intracellularly immunostained parasites was performed in order to evaluate population heterogeneity. Respective mean fluorescence index values of cells obtained with p*Tc*T2A-*actin*-HA and p*Tc*EndoT2A-*actin*-HA were 2.4 and 1.7-fold higher than that determined for wild type epimastigotes (Fig. S1A). Due to the overall low fluorescence and little signal difference, this approach proved unsuitable to establish the percentage of cells expressing the tagged genes. Nevertheless, immunofluorescence microscopy showed that >96 % of both types of parasites expressed the actin-HA fusion protein (Fig. 6E and Figs. S1B and C). Furthermore, thorough inspection of the cells revealed that the localization pattern of this recombinant protein was in close agreement with that previously reported for endogenous untagged actin (Fig. 6E) [39].

To test if the *actin* gene could be tagged reproducibly in another strain a similar approach was conducted with Y strain epimastigotes. According to the Tritryp database, Y and Dm28c *actin* gene orthologs display several single nucleotide polymorphisms (SNPs) throughout their length. Consequently, accurate insertion of the tagging construct should produce a hybrid *actin* coding sequence with Y and Dm28c strain specific SNPs at the 5′ and 3′ end respectively. Endogenous tagging of the *actin* locus in the resulting Y strain transgenic parasite population was analyzed by Western blot analysis (Fig. S2) and genomic DNA was used as template to amplify the expected hybrid *actin* gene. The resulting amplicon was submitted for sequencing along with equivalents derived from wild type Y and Dm28c strains obtained for comparison purposes. As expected, the section upstream the *Hind*III site used for linearization of the tagging construct contained Y strain specific SNPs while those identified in the downstream region corresponded to SNPs of the Dm28c strain (Fig. S2). These results confirmed that the endogenous tagging of the *actin* gene had indeed taken place by homologous ends-in recombination.

3. Discussion

This study was aimed at the development of a simple genetic manipulation strategy based on 2A sequences which enabled the expression of multiple polypeptides from a single mRNA in *T. cruzi* and thus reducing the dependence on multiple and different intergenic regions to express the sequences of interest as well as the selectable marker. This was accomplished using a single DNA molecule containing both sequences linked in frame by that for the T2A peptide. This design, which included a minimum set of regulatory components, offers several advantages; (i) 2A sequences are shorter (≈60 bp) compared with conventional trypanosomatid intergenic regions (>180 bp), (ii) it could potentially be used for the expression of multiple proteins from a single coding sequence by including several 2A elements such as has been done in other model organisms and, (iii) improves the selection of heterologous transgenes hence assisting with additional cloning steps. In this sense, this is a substantial advantage since enrichment strategies such as dilution cloning, or cell sorting approaches are technically challenging given that not all *T. cruzi* strains are easily cloneable.

Transgenic epimastigotes obtained using the T2A based single mRNA vector and the more conventional two-mRNA derivative reached similar mEGFP expression levels and, especially for Dm28c and Y strains, cell populations displayed remarkable homogeneity. In most cases, both plasmid configurations could be suitable for transgene expression in *T. cruzi*. Nevertheless, p*Tc*T2A-Neo out-performed p*Tc*G-Neo since, independently of the strain used, it allowed to obtain higher fractions of mEGFP positive cells with fewer passages and a shorter time in culture. So far in this work only *actin* gene overexpression was evaluated employing a T2A based strategy. Further experimentation with the expression of additional *T. cruzi* endogenous genes will be required to fully understand the potential applications of this element.

Poor 2A peptide processing and inefficient antibiotic resistant protein dissociation has been linked to problematic selection [40]. In this regard, T2A self-cleavage activity was greater than 80 % for all fusion proteins analyzed in epimastigote stage while unprocessed fusion products remained undetectable in mammalian host associated forms. These observed high efficiencies, equivalent to those reported for endogenous viral-like self-cleaving 2A sequences from *T. cruzi* L1Tc non-LTR retrotransposons [26], likely allow effective G418-based positive selection as well as appropriate gene of interest expression. In fact, from all available well characterized 2A peptides [41] the T2A sequence was chosen in this work for having the highest sequence similarity to the endogenous viral-like self-cleaving 2A (Fig. S3).

The CRISPR/Cas9 technology has been successfully used to produce knockout and endogenously tagged cell lines in *T. cruzi* [13]. Nevertheless, most popular Cas9 based techniques require preestablished cells lines that constitutively express the nuclease, limiting the number of strains on which these techniques can be applied [42,43]. Alternative strategies that overcome this limitation have been described however these approaches are technically challenging and involve the transfection of purified recombinant Cas9 ribonu-cleoprotein with an *in vitro* transcribed sgRNA [36]. Given the high proportion of transgenic parasites expressing the mEGFP reporter in the population obtained with the 2A based vectors developed in this work, it was considered to modify these plasmids to facilitate the endogenous tagging of genes without requiring the use of exogenous nucleases. Simply removing 5′ end regulatory elements from p*Tc*T2A-*actin*-HA, resulted in a construct capable of producing a population with over 96 % of the cells displaying a HA tagged *actin* gene. With the same strategy larger tags such as mEGFP, were also efficiently integrated into de *actin* locus, even though, the actin-mEGFP fusion protein accumulated at the posterior end of the parasite colocalizing with *Tc*CBP, a reservosome-resident serine carboxypeptidase [44] (Fig. S4). In this respect, the miss incorporation of actin-mEGFP monomers into filaments has already been reported in other model systems [45].

Insertion of p*Tc*EndoT2A derived constructs into genomic loci occurs by ends-in homologous recombination and results in a tandem duplication of the target sequence. In *T. cruzi* only a few expression vectors make use of this integration strategy such as pROCKGFPNeo [9] and its derivatives. In contrast, ends-in homologous recombination is among the most frequently used method for the insertion of parasite-derived or foreign DNA sequences into different locations, or to provide novel regulation of parasite gene expression in *T. brucei* [38]. Like other alternative tagging systems, insertion of p*Tc*EndoT2A based constructs will modify the 3′ UTR of the gene of interest and therefore, most likely the endogenous regulation patterns. Genetic manipulation of *T. cruzi* is most frequently performed in the epimastigote replicative stage. Therefore, the inclusion of histone H4 intergenic sequence allows to target, for endogenous tagging, any gene of interest even those that are not physiologically expressed in the insect form such as several mammalian host-associated virulence factors [46–48].

Despite the versatility of the 2A peptide-based systems, some limitations are worth mentioning. First, 2A remnants at the C-terminal end may have potential deleterious effects on the target protein or affect their subcellular localization [49]. On the other hand, some specific 2A peptide-selectable marker configurations have been shown not to confer appropriate antibiotic resistance such as the neomycin resistance gene positioned after the sequence for the porcine teschovirus-1 2A (P2A) in *Dictyostelium discoideum* cells [50]. For these reasons and given that 2A peptides differ in length and sequence, a careful design of 2A fusion constructs as well as the optional insertion of linker sequences [51], may be key aspects to improve protein expression, cleavage efficiency and consequently, the selection process. Taking these facts into consideration, 2A peptides are valuable additions to the genetic manipulation toolbox in *T. cruzi*.

4. Materials and methods

4.1. Animal assays, protein expression and ethics statement

The protocol of animal immunization procedures followed in this study was approved by the Ethics Committee of Animal Ex-periments of the Universidad Nacional de San Martín (CICUAE N° 08/2015) and according to the recommendations of the Guide for

the Care and Use of Laboratory Animals of the National Institutes of Health. To produce antibodies against neomycin phosphotransferase (Neo, G418 resistant marker), the gene was cloned into the pET-22b (+) (Novagen-Millipore Sigma, Burlington, MA, USA) derived pTac22 plasmid, expressed in *E. coli* BL-21 (DE3) with an N-terminal hexahistidine tag, and purified by HisTrap HP Cytiva following manufacturer's procedures. Mice received three doses of recombinant neomycin phosphotransferase emulsified in Freund's adjuvant 14 days apart and bled 14 days after the last dose.

4.2. Plasmid design

Construction of p*Tc*T2A-Neo and p*Tc*G-Neo was accomplished combining several amplicons obtained by PCR. Each fragment cloned into pGEM-T Easy (Promega Corporation, Madison, WI, USA) was verified by Sanger sequencing (Macrogen, Seoul, Korea). Segments corresponding to the ribosomal promoter and HX1 region were obtained from pTREX vector [7] while histone H4 intergenic sequence was amplified using Dm28c strain genomic DNA as template. The Neo G418 resistance gene was derived from plasmid p*Tc*R-GA Neo + [10] while the sequence coding the N-terminal T2A peptide was added to the primer as a 5′ extension. Similarly, the section encompassing the *GAPDH* intergenic sequence and *G418* resistance gene was isolated employing pTREX as template [52]. The sequences of p*Tc*T2A-Neo and p*Tc*G-Neo were deposited in GenBank under accession numbers OR453403 and OR453404 respectively.

For the nuclear localization of green fluorescent protein, the *mEGFP* gene was amplified with primers containing extensions corresponding to the coding sequences for the *T. cruzi* La protein NLS [37] and the resulting fragments were inserted into p*Tc*T2A-Neo and p*Tc*G-Neo replacing the sequence for the cytosolic mEGFP variant.

For the ectopic overexpression of the *actin* gene, the corresponding full length coding sequence was amplified with primers CCATGGGTTCTGACGAAGAACAGTCCGCTATTG and GATATCACTAGTAAAGCATTTGTTGTGCACAATGCTTG using Dm28c strain genomic DNA as template and inserted into p*Tc*T2A-Neo fused to the sequences for a C-terminal HA epitope tag or cytosolic mEGFP producing p*Tc*T2A-*actin*-HA and p*Tc*T2A-*actin*-mEGFP. To obtain derivatives for the endogenous tagging of the *actin* gene, fragments corresponding to the 874 bp 3′ section of the *actin* gene, the sequence for the HA epitope or mEGFP tag as well as the T2A-Neo coding and histone H4 intergenic sequences were obtained by *Bgl*II-*Kpn*I digestion and inserted into BamHI-*Kpn*I treated pBlueScript II KS (+). The resulting vectors lacked 5′ promoter and regulatory sequences as well as the 257 bp initial section of the *actin* gene. The unique *Hin*dIII site used for linearization prior to transfection could be found inside the remaining *actin* coding sequence.

Recombinant endogenous tagged *actin* loci were PCR amplified with primers ATGTCTGACGAAGAACAGTCCGCTATTG (A$_{fw}$) and GGGGCCCCGGATTCTCCTCGACGTCACCGCA (T2A$_{rv}$). Likewise, control WT *actin* coding sequences were obtained from Dm28c and Y strain genomic DNA with primers A$_{fw}$ and AAAGCATTTGTTGTGCACAATGCTTG (A$_{rv}$). Amplicons were submitted to Macrogen for sequencing with primers AGAAGCTTTTTGTTGGCGAC (actSeq$_{fw}$) and AGGTGCAAGGTTGCTGATCTC (actSeq$_{rv}$).

4.3. Trypanosome culture

Epimastigotes of the Dm28c, Sylvio-X10 and Y strains were cultured in brain-heart infusion-tryptose culture medium (BHT) supplemented with 10 % fetal bovine serum at 28 °C [53]. Vero cell monolayers were grown in minimal essential medium Eagle (Gibco, Carlsbad, CA, USA) supplemented with 5 % (v/v) fetal bovine serum. Vero cells were initially infected with transgenic metacyclic trypomastigotes obtained by spontaneous differentiation from late-stationary phase cultured epimastigotes (first passage).

4.4. Transgenic epimastigote cell line obtention

Approximately 1.5×10^8 mid-log phase epimastigotes ($\sim 40 \times 10^6$ parasites/mL) were collected, washed twice with BHT, and resuspended in serum-free medium. For each transfection, 10–20 μg of plasmid was added to 350 μL of the parasite suspension and the entire cell-DNA mixture was immediately electroporated in a 0.2 cm electroporation cuvette with a single pulse administered using a BTX 600 Electro Cell Manipulator (BTX Inc., San Diego, CA, USA) with parameters set to 335 V, 1400 μF and 24 Ω resistance. Parasites were selected with 200 μg/mL of G418 (InvivoGen) in BHT medium supplemented with 20 % fetal bovine serum.

4.5. Isolation of trypomastigotes and intracellularly derived amastigotes

Cell-derived trypomastigotes were purified from the supernatants of infected Vero cells monolayers. Briefly, 7 days post infection, the supernatants were transferred to round-bottom centrifuge tubes (Oak Ridge Style) and centrifuged at 1600×*g* for 10 min. Highly motile trypomastigotes were then recovered following a swim out procedure for 3 h at 37 °C in a 5 % CO$_2$ incubator prior to collection and washing in PBS.

To obtain intracellularly derived amastigotes, 72-h-infected Vero cells were washed twice with PBS (to remove trypomastigotes and extracellular amastigotes) and mechanically detached from culture flasks using a cell scraper. The resulting cell suspension was passed at least 3 times through a syringe with a 25G needle followed by a similar procedure using a 30G needle in order to lyse the host cells and release the intracellular amastigotes. Unbroken Vero cells and debris were removed by centrifugation at 180×*g* for 5 min.

4.6. Electrophoresis and immunoblotting

Parasites were resuspended in 1X Laemmli sample buffer and boiled for 5 min. Samples were loaded on Tris-glycine SDS-polyacrylamide gels (10 or 12.5 % acrylamide) and then transferred to a nitrocellulose membrane (Hybond ECL, GE Healthcare, Pittsburgh,

PA, USA). Blots were probed with monoclonal anti GFP mouse clones 7.1 and 13.1 antibody diluted 1:1000 (Sigma-Aldrich), anti HA High Affinity (clone 3F10) 1:1000 (Roche, Mannheim, Germany) or anti α-tubulin 1:5000 clone B-5-1-2 (Sigma-Aldrich) antibodies. Polyclonal anti G418 serum was raised in mice (1:500). Alexa Fluor 680 AffiniPure Goat Anti-Mouse IgG (H + L), Alexa Fluor 790 AffiniPure Goat Anti-Mouse IgG (H + L) and Alexa Fluor 790 AffiniPure Goat Anti-Rat IgG (H + L) secondary antibodies were purchased from Jackson Immunoresearch Laboratories (West Grove, PA, USA). The membranes were visualized with an Odyssey laser scanning system and analyzed with Image Studio software (LI-COR Biosciences, Lincoln, NE, USA). The PageRuler™ Prestained Protein Ladder was obtained from Pierce (Rockford, IL, USA).

4.7. Fluorescence microscopy

For fluorescence microscopy of mEGFP, parasites were fixed with 4 % paraformaldehyde in PBS, washed twice with PBS, and then adhered to poly-L-lysine coated coverslips. For immunofluorescence assays, fixed parasites were blocked and permeabilized with 2.5 % BSA, 2.5 % horse serum and 0.5 % saponin in PBS for 1 h, and then probed with Anti HA High Affinity (1:1000) or rabbit anti-serine carboxypeptidase (1:2000) [44] antibodies. Alexa Fluor 488 Goat anti-rat IgG or Alexa Fluor 568 Goat anti-rabbit IgG (Invitrogen, 1:1000) were used as secondary antibodies. Nuclear and kinetoplast DNA was stained with 4′,6-diamidino-2-phenylindole (DAPI). Fluorescence was monitored with an Eclipse 80i or (Eclipse) E600 microscope (Nikon, Shinagawa, Japan).

4.8. Flow cytometry

Mid-log phase density epimastigotes fixed with 4 % paraformaldehyde solution in PBS. Fluorescence was read with a CyFlow space cytometer (Partec, Germany), and data was analyzed employing the FlowJo VX0.7 software (FlowJo LLC, Ashland, OR USA).

Funding

CRediT authorship contribution statement

Gabriela T. Niemirowicz: Writing – review & editing, Writing – original draft, Investigation, Funding acquisition, Formal analysis, Conceptualization. **Giannina Carlevaro:** Investigation. **Oscar Campetella:** Resources, Funding acquisition, Formal analysis. **León A. Bouvier:** Writing – review & editing, Writing – original draft, Investigation, Formal analysis, Conceptualization. **Juan Mucci:** Writing – review & editing, Writing – original draft, Supervision, Project administration, Investigation, Funding acquisition, Conceptualization.

Declaration of competing interest

The authors declare that they have no known competing financial interests or personal relationships that could have appeared to influence the work reported in this paper.

Acknowledgments

Appendix A. Supplementary data

Supplementary data to this article can be found online at https://doi.org/10.1016/j.heliyon.2024.e24595.

References

[1] C.E. Clayton, Gene expression in kinetoplastids, Curr. Opin. Microbiol. 32 (2016) 46–51, https://doi.org/10.1016/J.MIB.2016.04.018.
[2] J.H. LeBowitz, H.Q. Smith, L. Rusche, S.M. Beverley, Coupling of poly(A) site selection and *trans*-splicing in *Leishmania*, Genes Dev. 7 (1993) 996–1007, https://doi.org/10.1101/GAD.7.6.996.
[3] K.R. Matthews, C. Tschadi, E. Ullu, A common pyrimidine-rich motif governs *trans*-splicing and polyadenylation of tubulin polycistronic pre-mRNA in trypanosomes, Genes Dev. 8 (1994) 491–501, https://doi.org/10.1101/GAD.8.4.491.

[4] J.G. De Gaudenzi, G. Noé, V.A. Campo, A.C. Frasch, A. Cassola, Gene expression regulation in trypanosomatids, Essays Biochem. 51 (2011) 31–46, https://doi.org/10.1042/BSE0510031.

[5] J.M. Kelly, H.M. Ward, M.A. Miles, G. Kendall, A shuttle vector which facilitates the expression of transfected genes in *Trypanosoma cruzi* and *Leishmania*, Nucleic Acids Res. 20 (1992) 3963–3969, https://doi.org/10.1093/NAR/20.15.3963.

[6] S. Martínez-Calvillo, I. López, R. Hernández, pRIBOTEX expression vector: a pTEX derivative for a rapid selection of *Trypanosoma cruzi* transfectants, Gene 199 (1997) 71–76, https://doi.org/10.1016/S0378-1119(97)00348-X.

[7] M.P. Vazquez, M.J. Levin, Functional analysis of the intergenic regions of TcP2β gene *loci* allowed the construction of an improved *Trypanosoma cruzi* expression vector, Gene 239 (1999) 217–225, https://doi.org/10.1016/S0378-1119(99)00386-8.

[8] H.A. Lorenzi, M.P. Vazquez, M.J. Levin, Integration of expression vectors into the ribosomal locus of *Trypanosoma cruzi*, Gene 310 (2003) 91–99, https://doi.org/10.1016/S0378-1119(03)00502-X.

[9] W.D. DaRocha, R.A. Silva, D.C. Bartholomeu, S.F. Pires, J.M. Freitas, A.M. Macedo, et al., Expression of exogenous genes in *Trypanosoma cruzi:* improving vectors and electroporation protocols, Parasitol. Res. 92 (2004) 113–120, https://doi.org/10.1007/S00436-003-1004-5.

[10] L.A. Bouvier, M. de los M. Cámara, G.E. Canepa, M.R. Miranda, C.A. Pereira, Plasmid vectors and molecular building blocks for the development of genetic manipulation tools for *Trypanosoma cruzi*, PLoS One 8 (2013) 80217, https://doi.org/10.1371/JOURNAL.PONE.0080217.

[11] L.M. Wen, P. Xu, G. Benegal, M.R.C. Carvaho, D.R. Butler, G.A. Buck, *Trypanosoma cruzi*: exogenously regulated gene expression, Exp. Parasitol. 97 (2001) 196–204, https://doi.org/10.1006/EXPR.2001.4612.

[12] M.C. Taylor, J.M. Kelly, pTcINDEX: a stable tetracycline-regulated expression vector for *Trypanosoma cruzi*, BMC Biotechnol. 6 (2006), https://doi.org/10.1186/1472-6750-6-32.

[13] N. Lander, M.A. Chiurillo, State-of-the-art CRISPR/Cas9 technology for genome editing in trypanosomatids, J. Eukaryot. Microbiol. 66 (2019) 981–991, https://doi.org/10.1111/JEU.12747.

[14] D. Peng, S.P. Kurup, P.Y. Yao, T.A. Minning, R.L. Tarleton, CRISPR-Cas9-mediated single-gene and gene family disruption in *Trypanosoma cruzi*, mBio 6 (2014), https://doi.org/10.1128/MBIO.02097-14.

[15] J.I. MacRae, S.O. Obado, D.C. Turnock, J.R. Roper, M. Kierans, J.M. Kelly, et al., The suppression of galactose metabolism in *Trypanosoma cruzi* epimastigotes causes changes in cell surface molecular architecture and cell morphology, Mol. Biochem. Parasitol. 147 (2006) 126–136, https://doi.org/10.1016/J.MOLBIOPARA.2006.02.011.

[16] M.S. Cardoso, C. Junqueira, R.C. Trigueiro, H. Shams-Eldin, C.S. Macedo, P.R. Araújo, et al., Identification and functional analysis of *Trypanosoma cruzi* genes that encode proteins of the glycosylphosphatidylinositol biosynthetic pathway, PLoS Neglected Trop. Dis. 7 (2013), https://doi.org/10.1371/JOURNAL.PNTD.0002369.

[17] C.P. Brandan, A.M. Padilla, D. Xu, R.L. Tarleton, M.A. Basombrio, Knockout of the *dhfr-ts* gene in *Trypanosoma cruzi* generates attenuated parasites able to confer protection against a virulent challenge, PLoS Neglected Trop. Dis. 5 (2011), https://doi.org/10.1371/JOURNAL.PNTD.0001418.

[18] A.J. Roberts, L.S. Torrie, S. Wyllie, A.H. Fairlamb, Biochemical and genetic characterization of *Trypanosoma cruzi* N-myristoyltransferase, Biochem. J. 459 (2014) 323–332, https://doi.org/10.1042/BJ20131033.

[19] M.L.L. Donnelly, G. Luke, A. Mehrotra, X. Li, L.E. Hughes, D. Gani, et al., Analysis of the aphthovirus 2A/2B polyprotein "cleavage" mechanism indicates not a proteolytic reaction, but a novel translational effect: a putative ribosomal "skip.", J. Gen. Virol. 82 (2001) 1013–1025, https://doi.org/10.1099/0022-1317-82-5-1013.

[20] J.F. Atkins, N.M. Wills, G. Loughran, C.Y. Wu, K. Parsawar, M.D. Ryan, et al., A case for "StopGo": reprogramming translation to augment codon meaning of GGN by promoting unconventional termination (Stop) after addition of glycine and then allowing continued translation (Go), RNA 13 (2007) 803–810, https://doi.org/10.1261/RNA.487907.

[21] J. Chng, T. Wang, R. Nian, A. Lau, K.M. Hoi, S.C.L. Ho, et al., Cleavage efficient 2A peptides for high level monoclonal antibody expression in CHO cells, mAbs 7 (2015) 403–412, https://doi.org/10.1080/19420862.2015.1008351.

[22] J. Fang, J.J. Qian, S. Yi, T.C. Harding, G.H. Tu, M. VanRoey, et al., Stable antibody expression at therapeutic levels using the 2A peptide, Nat. Biotechnol. 23 (2005) 584–590, https://doi.org/10.1038/NBT1087.

[23] A.L. Szymczak, C.J. Workman, Y. Wang, K.M. Vignali, S. Dilioglou, E.F. Vanin, et al., Correction of multi-gene deficiency in vivo using a single "self-cleaving" 2A peptide-based retroviral vector, Nat. Biotechnol. 22 (2004) 589–594, https://doi.org/10.1038/NBT957.

[24] S.H. Ha, Y.S. Liang, H. Jung, M.J. Ahn, S.C. Suh, S.J. Kweon, et al., Application of two bicistronic systems involving 2A and IRES sequences to the biosynthesis of carotenoids in rice endosperm, Plant Biotechnol. J. 8 (2010) 928–938, https://doi.org/10.1111/J.1467-7652.2010.00543.X.

[25] Y.S. Jeong, H.K. Ku, Y.J. Jung, J.K. Kim, K.B. Lee, J.K. Kim, et al., 2A-linked bi-, tri-, and quad-cistrons for the stepwise biosynthesis of β-carotene, zeaxanthin, and ketocarotenoids in rice endosperm, Metab Eng Commun 12 (2021) e00166, https://doi.org/10.1016/J.MEC.2021.E00166.

[26] S.R. Heras, M.C. Thomas, M. García-Canadas, P. De Felipe, J.L. García-Pérez, M.D. Ryan, et al., L1Tc non-LTR retrotransposons from *Trypanosoma cruzi* contain a functional viral-like self-cleaving 2A sequence in frame with the active proteins they encode, Cell. Mol. Life Sci. 63 (2006) 1449–1460, https://doi.org/10.1007/S00018-006-6038-2.

[27] M.S. Bertolini, M.A. Chiurillo, N. Lander, A.E. Vercesi, R. Docampo, MICU1 and MICU2 play an essential role in mitochondrial Ca^{2+} uptake, growth, and infectivity of the human pathogen *Trypanosoma cruzi*, mBio 10 (2019), https://doi.org/10.1128/MBIO.00348-19.

[28] P.C. Dumoulin, J. Vollrath, M.M. Won, J.X. Wang, B.A. Burleigh, Endogenous sterol synthesis is dispensable for *Trypanosoma cruzi* epimastigote growth but not stress tolerance, Front. Microbiol. 13 (2022) 937910, https://doi.org/10.3389/FMICB.2022.937910/FULL.

[29] L. Pagura, P.C. Dumoulin, C.C. Ellis, M.T. Mendes, I.L. Estevao, I.C. Almeida, et al., Fatty acid elongases 1-3 have distinct roles in mitochondrial function, growth, and lipid homeostasis in *Trypanosoma cruzi*, J. Biol. Chem. (2023) 299, https://doi.org/10.1016/J.JBC.2023.104715.

[30] F.M. Pringle, K.H.J. Gordon, T.N. Hanzlik, J. Kalmakoff, P.D. Scotti, V.K. Ward, A novel capsid expression strategy for *Thosea asigna* virus (*Tetraviridae*), J. Gen. Virol. 80 (Pt 7) (1999) 1855–1863, https://doi.org/10.1099/0022-1317-80-7-1855.

[31] B. Zingales, S.G. Andrade, M.R.S. Briones, D.A. Campbell, E. Chiari, O. Fernandes, et al., A new consensus for *Trypanosoma cruzi* intraspecific nomenclature: second revision meeting recommends TcI to TcVI, Mem. Inst. Oswaldo Cruz 104 (2009) 1051–1054, https://doi.org/10.1590/S0074-02762009000700021.

[32] M.S.M. Bertelli, Z. Brener, Infection of tissue culture cells with bloodstream trypomastigotes of *Trypanosoma cruzi*, J. Parasitol. 66 (1980) 992–997, https://doi.org/10.2307/3280403.

[33] M.G. Risso, G.B. Garbarino, E. Mocetti, O. Campetella, S.M. González Cappa, C.A. Buscaglia, et al., Differential expression of a virulence factor, the *trans*-sialidase, by the main *Trypanosoma cruzi* phylogenetic lineages, J. Infect. Dis. 189 (2004) 2250–2259, https://doi.org/10.1086/420831.

[34] R.C. Melo, Z. Brener, Tissue tropism of different *Trypanosoma cruzi* strains, J. Parasitol. 64 (1978) 475–482, https://doi.org/10.2307/3279787.

[35] S. Revollo, B. Oury, A. Vela, M. Tibayrenc, D. Sereno, *In vitro* benznidazole and nifurtimox susceptibility profile of *Trypanosoma cruzi* strains belonging to discrete typing units TcI, TcII, and TcV, Pathogens 8 (2019), https://doi.org/10.3390/PATHOGENS8040197.

[36] L.C.S. Medeiros, L. South, D. Peng, J.M. Bustamante, W. Wang, M. Bunkofske, et al., Rapid, selection-free, high-efficiency genome editing in Protozoan parasites using CRISPR-cas9 ribonucleoproteins, mBio 8 (2017), https://doi.org/10.1128/MBIO.01788-17.

[37] M.A. Marchetti, C. Tschudi, H. Kwon, S.L. Wolin, E. Ullu, Import of proteins into the trypanosome nucleus and their distribution at karyokinesis, J. Cell Sci. 113 (Pt 5) (2000) 899–906, https://doi.org/10.1242/JCS.113.5.899.

[38] R. McCulloch, E. Vassella, P. Burton, M. Boshart, J.D. Barry, Transformation of monomorphic and pleomorphic *Trypanosoma brucei*, Methods Mol. Biol. 262 (2004) 53–86, https://doi.org/10.1385/1-59259-761-0:053.

[39] A. Vizcaíno-Castillo, J.F. Osorio-Méndez, J.R. Ambrosio, R. Hernández, A.M. Cevallos, The complexity and diversity of the actin cytoskeleton of trypanosomatids, Mol. Biochem. Parasitol. 237 (2020), https://doi.org/10.1016/J.MOLBIOPARA.2020.111278.

[40] M. González, I. Martín-Ruíz, S. Jiménez, L. Pirone, R. Barrio, J.D. Sutherland, Generation of stable *Drosophila* cell lines using multicistronic vectors, Sci. Rep. 1 (2011), https://doi.org/10.1038/SREP00075.

[41] G.A. Luke, M.D. Ryan, Therapeutic applications of the 'NPGP' family of viral 2As, Rev. Med. Virol. 28 (2018) e2001, https://doi.org/10.1002/RMV.2001.

[42] F.C. Costa, A.F. Francisco, S. Jayawardhana, S.G. Calderano, M.D. Lewis, F. Olmo, et al., Expanding the toolbox for *Trypanosoma cruzi*: a parasite line incorporating a bioluminescence-fluorescence dual reporter and streamlined CRISPR/Cas9 functionality for rapid *in vivo* localisation and phenotyping, PLoS Neglected Trop. Dis. 12 (2018), https://doi.org/10.1371/JOURNAL.PNTD.0006388.

[43] N. Lander, Z.H. Li, S. Niyogi, R. Docampo, CRISPR/Cas9-Induced disruption of paraflagellar rod protein 1 and 2 genes in *Trypanosoma cruzi* reveals their role in flagellar attachment, mBio 6 (2015), https://doi.org/10.1128/MBIO.01012-15.

[44] C. Sant'Anna, F. Parussini, D. Lourenço, W. De Souza, J.J. Cazzulo, N.L. Cunha-E-Silva, All *Trypanosoma cruzi* developmental forms present lysosome-related organelles, Histochem. Cell Biol. 130 (2008) 1187–1198, https://doi.org/10.1007/S00418-008-0486-8.

[45] M. Melak, M. Plessner, R. Grosse, Actin visualization at a glance, J. Cell Sci. 130 (2017) 525–530, https://doi.org/10.1242/JCS.189068.

[46] O. Campetella, C.A. Buscaglia, J. Mucci, M.S. Leguizamón, Parasite-host glycan interactions during *Trypanosoma cruzi* infection: *trans*-Sialidase rides the show, Biochim. Biophys. Acta, Mol. Basis Dis. (2020) 1866, https://doi.org/10.1016/J.BBADIS.2020.165692.

[47] C.A. Buscaglia, V.A. Campo, A.C.C. Frasch, J.M. Di Noia, *Trypanosoma cruzi* surface mucins: host-dependent coat diversity, Nat. Rev. Microbiol. 4 (2006) 229–236, https://doi.org/10.1038/NRMICRO1351.

[48] C. Oliveira, F.B. Holetz, L.R. Alves, A.R. Ávila, Modulation of virulence factors during *Trypanosoma cruzi* differentiation, Pathogens 12 (2022), https://doi.org/10.3390/PATHOGENS12010032.

[49] H. Sun, N. Zhou, H. Wang, D. Huang, Z. Lang, Processing and targeting of proteins derived from polyprotein with 2A and LP4/2A as peptide linkers in a maize expression system, PLoS One 12 (2017), https://doi.org/10.1371/JOURNAL.PONE.0174804.

[50] X. Zhu, C. Ricci-Tam, E.R. Hager, A.E. Sgro, Self-cleaving peptides for expression of multiple genes in *Dictyostelium discoideum*, PLoS One 18 (2023), https://doi.org/10.1371/JOURNAL.PONE.0281211.

[51] J.H. Kim, S.R. Lee, L.H. Li, H.J. Park, J.H. Park, K.Y. Lee, et al., High cleavage efficiency of a 2A peptide derived from porcine teschovirus-1 in human cell lines, zebrafish and mice, PLoS One 6 (2011), https://doi.org/10.1371/JOURNAL.PONE.0018556.

[52] G.T. Niemirowicz, J.J. Cazzulo, V.E. Álvarez, L.A. Bouvier, Simplified inducible system for *Trypanosoma brucei*, PLoS One 13 (2018), https://doi.org/10.1371/JOURNAL.PONE.0205527.

[53] J.J. Cazzulo, B.M. Franke de Cazzulo, J.C. Engel, J.J.B. Cannata, End products and enzyme levels of aerobic glucose fermentation in trypanosomatids, Mol. Biochem. Parasitol. 16 (1985) 329–343, https://doi.org/10.1016/0166-6851(85)90074-X.

[54] R.L.S. Neris, A. Kaur, A.V. Gomes, Incorrect molecular weights due to inaccurate prestained protein molecular weight markers that are used for gel electrophoresis and western blotting, bioRxiv (2020), https://doi.org/10.1101/2020.04.03.023465, 2020.04.03.023465.